

Selective production of diethyl maleate *via* oxidative cleavage of lignin aromatic unit

Zhenping Cai^{1#}, Jinxing Long^{1#}, Yingwen Li¹, Lin Ye², Biaolin Yin¹, Liam John France¹, Juncai Dong³,
Lirong Zheng³, Hongyan He⁴, Sijie Liu¹, Shik Chi Edman Tsang^{2*} and Xuehui Li^{1*}

¹School of Chemistry and Chemical Engineering, State Key Laboratory of Pulp & Paper Engineering, South China University of Technology, Guangzhou 510640, China

²Wolfson Catalysis, Inorganic Chemistry Laboratory, University of Oxford, Oxford, OX1 3QR, UK

³Beijing Synchrotron Radiation Facility, Institute of High Energy Physics, Chinese Academy of Sciences, Beijing 100049, China

⁴Beijing Key Laboratory of Ionic Liquids Clean Process, Institute of Process Engineering, Chinese Academy of Sciences, Beijing 100190, China

[#]These authors contributed equally to this work

*Correspondence: edman.tsang@chem.ox.ac.uk; cexhli@scut.edu.cn

SUMMARY

Green production of bulk chemicals traditionally obtained from fossil resources is of great importance. One potential route towards realizing this goal is through the utilization of renewable lignin, however, current techniques generally lead to low product specificity due to the structural diversity of this recalcitrant biopolymer. Herein, we devised a new catalytic system to promote selectively oxidative lignin in air. Diethyl maleate is formed at impressively high yield of 404.8 mg g⁻¹ and selectivity of 72.7% over the polyoxometalate ionic liquids of [BSmim]CuPW₁₂O₄₀. This high catalytic activity is ascribed to five-coordinated Cu⁺ species, which, through the formation of end-on dioxygen species in vacant orbitals, facilitates the selective oxidation of basic lignin aromatic units (phenylpropane C₉ units). Therefore, these results represent significant progress

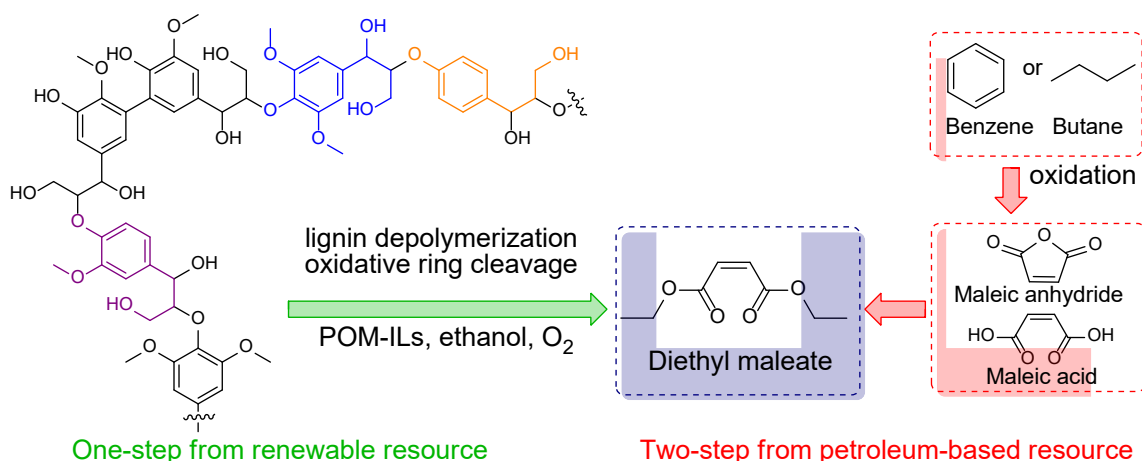
towards the realization of an industrially applicable and highly selective lignin oxidation process for the generation of value-added and bulk chemicals.

Introduction

Lignin, as the major component of lignocellulosic biomass in nature (15~30% by weight), is an ideal renewable feedstock for production of platform chemicals.¹⁻⁴ Especially, this natural polymer is a kind of high-volume ‘waste’ in pulp and paper industry and modern bio-refinery processes.^{5, 6} If converted to useful chemicals traditionally obtained from fossil resources, this can bring huge benefits to chemical industry and environment. However, the efficient lignin utilization is a big challenge and has long been recognized as the bottleneck in the biomass valorization, mainly due to its complex molecular structure and highly recalcitrant chemical nature.^{7, 8} For example, less than 2% of lignin is currently utilized and most of it is directly burned for the internal energy.⁹ To date, depolymerization technologies such as hydrogenolysis, alcoholysis, pyrolysis, liquefaction, and oxidation are widely reported in research laboratories for the transformation of lignin into fine chemicals or biofuel.^{9, 10} For example, carboxyl acids such as formic acid, acetic acid and unsaturated dicarboxylic acids could be obtained from the oxidation of lignin and model compounds.¹¹ On the other hand, development of these catalytic methods is severely limited by poor miscibility to lignin, uncontrolled oxidation to lead to a range of products and the formation of undesirable interunit carbon-carbon bonds generating more complex intermediates during processing. To overcome this problem, Shuai et al. used formaldehyde to block the reactive groups that would otherwise lead to carbon-carbon bonds during hydrogenolysis of lignin to produce improved yields of monomers.¹² Nevertheless, the general poor catalytic efficiencies and lack of product specificity for further processing render the conversion of lignin to useful chemicals very difficult for industrial practice.

Polyoxometalate catalysts are well known for their high redox activity and good stability over a

wide range of temperatures and pHs, which have also been previously studied for the delignification and transformation of lignin by breaking up its corresponding linkage bonds.^{13, 14} For example, Zhao et al. recently reported a novel polyoxometalates mediated biomass fuel cell which could directly convert lignin to electricity with high power output and Faradaic efficiency.¹⁵ However, development of an efficient catalyst is still of the key importance for the formation of value-added chemicals from the lignin. Considering the combined advantages of ionic liquid and polyoxometalate with the introduction of desirable acidity, reduction-oxidation and miscibility properties, we have designed a series of polyoxometalate-ionic liquid catalysts (POM-ILs, Scheme 1) for the selective oxidative cleavage of lignin basic aromatic units (phenylpropane units (C9 unit) to produce diethyl maleate (DEM) in ethanol. A typical result over our [BSmim]CuPW₁₂O₄₀ catalyst shows that 94.5% of wheat stalk lignin is consumed in a batch reactor to give 556.7 mg g⁻¹ volatile products which contain 72.7% selectivity towards DEM. DEM is an industrial important chemical and widely used in many fields such as polymers, spice and pesticide.¹⁶ More importantly, the use of DEM as platform chemicals from biomass for chemical industry is also feasible for its further conversions to maleic acid and its derivatives,¹⁷ high valued chemicals in petrochemical industry. Previously, DEM was produced *via* a two-step process of benzene (derived from petroleum) oxidation to maleic anhydride/maleic acid, followed by esterification with ethanol (Scheme 1).¹⁸ Due to rigid oxidation condition and serious pollution, the oxidation of butane (from petroleum refinery) is used as the alternative route, which represents for about 1.8 million tons/p.a. worldwide.¹⁹ However, the heavy dependence of fossil resources, high reaction temperature (673-723 K) and low process efficiency (70-85% conversion and 65-70% selectivity of maleic anhydride)²⁰ render this presently new selective renewable process competitive. The present process has a great potential in lignin valorization and sustainable DEM production for replacing the current petroleum-based technology.



Scheme 1. The novel renewable strategy from lignin oxidation (green) as compared to petroleum based process (red) for DEM production

POM-ILs: [BSmim]MPW₁₂O₄₀, BS= -CH₂CH₂CH₂CH₂SO₃H, M= Na, Mn, Co, Ni and Cu (Figure S1, the catalyst structure and properties characterization results are shown in Figure S2-S4, and Table S2-S5); the basic aromatic, phenylpropane units (C₉ unit) of lignin are marked

RESULT and DISCUSSION

Selective oxidation cleavage of lignin aromatic unit

We begin our study using an organosolv bagasse lignin, a typical herbaceous lignin containing all lignin phenylpropane units (C₉ unit) of *p*-coumaryl (H), coniferyl (G) and sinapyl (S) alcohols. No cleavage product of benzene ring units is detected in the absence of catalyst (Table 1, entry 1) although 48.2% of lignin is depolymerized with the formation of volatile aromatic compounds such as 4-hydroxybenzaldehyde and vanillin from the lignin aerobic oxidation (Table S6).²¹ A significant increase of lignin depolymerization is exhibited by the -SO₃H functionalized ionic liquid [BSmim]HSO₄ as acid is capable of catalyzing ether bond cleavage.²² However, only 6.5 and 15.9 mg g⁻¹ of DEM and C₄ esters from the benzene ring cleavages are detected, respectively, the C₄ esters are consisted of diethyl maleate, diethyl succinate, diethyl fumarate and diethyl malate, *etc* (Table 1, entry 2, and Table S6, Figure S5-S6, Table S7). It is interesting to see that a remarkable enhancement of lignin

Table 1. Selectively catalytic oxidation of bagasse lignin to DEM

| Entry | Catalysts | Solvent ^a | Conversion (%) | Yield of volatile product (mg g ⁻¹) | | | | Selectivity (%) ^d | |
|-----------------|--|----------------------|----------------|---|-----------------------------------|---------------------|--------|------------------------------|----------------------|
| | | | | DEM | C ₄ ester ^b | Others ^c | Total | DEM | C ₄ ester |
| 1 | — ^e | 80:20 | 48.2 | — | — | 14.7 | 14.7 | 0 | 0 |
| 2 | [BSmim]HSO ₄ | 80:20 | 82.4 | 6.5 | 15.9 | 32.2 | 48.1 | 13.5 | 33.1 |
| 3 | [BSmim]Na ₂ PW ₁₂ O ₄₀ | 80:20 | 81.3 | 53.6 | 59.8 | 9.3 | 69.1 | 77.6 | 86.5 |
| 4 | [BSmim]MnPW ₁₂ O ₄₀ | 80:20 | 80.9 | 87.7 | 107.6 | 22.7 | 130.3 | 67.3 | 82.6 |
| 5 | [BSmim]CoPW ₁₂ O ₄₀ | 80:20 | 80.6 | 93.3 | 105.6 | 40.9 | 146.5 | 63.7 | 72.1 |
| 6 | [BSmim]NiPW ₁₂ O ₄₀ | 80:20 | 84.3 | 100.4 | 116.0 | 50.3 | 166.3 | 60.4 | 69.8 |
| 7 | [BSmim]CuPW ₁₂ O ₄₀ | 80:20 | 90.7 | 153.6 | 176.2 | 82.9 | 259.1 | 59.3 | 68.0 |
| 8 ^f | [Bmim]CuPW ₁₂ O ₄₀ | 80:20 | 80.8 | 11.0 | 16.7 | 29.5 | 46.2 | 23.8 | 36.1 |
| 9 ^g | H ₂ SO ₄ /CuSO ₄ | 80:20 | 86.8 | 16.5 | 20.8 | 53.7 | 74.5 | 22.1 | 27.9 |
| 10 ^h | [BSmim]Na ₂ PW ₁₂ O ₄₀ /CuSO ₄ | 80:20 | 90.0 | 100.9 | 111.2 | 51.4 | 162.6 | 62.1 | 68.4 |
| 11 ⁱ | [BSmim]CuPW ₁₂ O ₄₀ | 80:20 | 31.3 | — | — | 78.6 | 78.6 | 0 | 0 |
| 12 | [BSmim]CuPW ₁₂ O ₄₀ | 100:0 | 92.9 | 274.7 | 310.9 | 87.5 | 398.4 | 69.0 | 78.0 |
| 13 ^j | [BSmim]CuPW ₁₂ O ₄₀ | 40:60 | 100.0 | 152.9 | 495.7 | — | 495.7 | 30.8 | 100.0 |
| 14 ⁱ | [BSmim]CuPW ₁₂ O ₄₀ | 80:20 | 100.0 | 416.3 | 489.0 | — | 489.0 | 85.1 | 100.0 |
| 15 ^j | [BSmim]CuPW ₁₂ O ₄₀ | 100:0 | 100.0 | 1111.5 | 1111.5 | — | 1111.5 | 100.0 | 100.0 |

Reaction conditions: 0.25 g bagasse lignin, 0.9 mmol catalyst, 20 mL ethanol-water mixture, 433 K, 5 h, 0.8 MPa O₂.

^a volume ratio of ethanol to water (v/v); ^b including diethyl maleate, diethyl succinate, diethyl fumarate, and diethyl malate; ^c in addition to C₄ ester of volatile products; ^d the selectivity of DEM is based on the volatile product determined by GC-MS-FID; ^e not added or detected; ^f the yield of volatile product was obtained by esterification of lignin depolymerization product (after removal of original solvent) with ethanol at 373 K for 2.0 h by adding 0.45 mmol H₂SO₄; ^g 0.45 mmol H₂SO₄ with 0.9 mmol CuSO₄; ^h adding 0.9 mmol CuSO₄; ⁱ using 0.8 MPa N₂; ^j 0.25 g maleic acid as substrate.

depolymerization and volatile products yield have been achieved when POM-IL ([BSmim]MPW₁₂O₄₀, M=Na⁺, Mn²⁺, Co²⁺, Ni²⁺ and Cu²⁺) is used as a catalyst (Table 1 and Table S6). The POM-IL is

composed of [BSmim]⁺ cation and [MPW₁₂O₄₀]⁻ polyoxometalate anion, which is known to form a reversible oxidant for one-electron transfer.²³ For example, 81.3% of bagasse lignin is depolymerized by [BSmim]Na₂PW₁₂O₄₀ with 69.1 mg g⁻¹ of volatile product yield, where 77.6% selectivity is towards the DEM product (Table 1, entry 3, the conversion of lignin/model compound, the yield and selectivity of products were calculated according to Eq. 1 to 4, *ESI*, using gas chromatography and excluding the oligomer section). As seen, the selectively oxidative cleavage of lignin aromatic unit is significantly promoted by the replacement of Na⁺ using typical low toxicity and non-expensive transition metal ions such as Mn²⁺, Co²⁺, Ni²⁺, and Cu²⁺ (Table 1, entries 4-7). Overall, [BSmim]CuPW₁₂O₄₀ shows the best activity, giving 90.7% of lignin depolymerization, 259.1 mg g⁻¹ yield of volatile products with 59.3% selectivity to DEM (Table 1, entry 7), suggesting that transition metal ion plays a key role in this process. In addition, above results clearly demonstrate that this novel process is highly selective for single chemical production (DEM) from the renewable lignin in comparison with current lignin depolymerization technologies.¹⁰

To obtain the probable reason for this high activity of POM-IL, several catalyst characterization techniques were conducted. As shown in Figure 1I and Figure S3, XRD clearly demonstrates the pattern with a space group of *Pcca* for the polyoxometalate structure where the Mⁿ⁺ can substitute into the octahedral W position. Our synchrotron PXRD study also illustrates the high crystallinity and purity of all the typical POM-ILs catalysts prepared for this study. For example, for typical CuPOM ([BSmim]CuPW₁₂O₄₀), the quality of the Le Bail refinement of synchrotron PXRD data from Diamond light source, UK has been assured with a low goodness-of-fit factor, a low weighted profile factor and a well fitted pattern (Figure S3B). The Le Bail refinement result clearly depicts that the common space group of the POM has been altered from *Pcca* to *Pncn* (Cu-POM) due to the structural distortion from the M substitution.²⁴⁻²⁶ The best fitting also suggests that there are two groups of closely related unit cell

parameters, presumably due to a slight difference in the CuPOM units packing (Table S2-S3). The unit cell volumes are 4856.1(1) Å³ for Cu-POM1 and 3068.1(1) Å³ for Cu-POM2, respectively. The distortion of the POM with the incorporation of Cu²⁺ ions can be appreciated by using the transformation matrix in WinGX with the input of the Le Bail profile refinement data as the distorted Cu-POM1 unit (Figure1I). The presentation of the full structural details in terms of atomic positions, connectivity or coordination geometry is also shown in Tables S2 and S3 by Rietveld refinement, following the initial model by Le Bail- WinGX. As seen from the refinement of CuPOM-IL using Rietveld method: after putting the above two groups of the structure and adding some free waters, the best fitting was obtained with the acceptable Rwp of 9.975, Rexp is 6.605 and gof of 1.510. As a result, the 4 original six-coordinated (6-CN) W/Cu as Keggin ion units have been distorted to form 5-CN W/Cu units in the general molecular formula (PW₁₂O₄₀)³⁻, the charge of which are counter-balanced by [BSmim] cations. In addition, the CuPOM anions are inter-connected through the corner sharing of μ-oxo ligands of the two 5-CN W/Cu sites due to condensation. Similar μ-oxo oligomers/polymers of W or V based POM structures have been reported.²⁷ It is important to establish the superior activity and selectivity with the Cu incorporation into this new catalyst system, and anticipated that the two remaining 5-CN Cu sites could be the active sites, which give vacant orbitals to take up the molecular oxygen as end-on species on Cu sites to approach the distorted near 6-CN sites for this oxidation reaction.

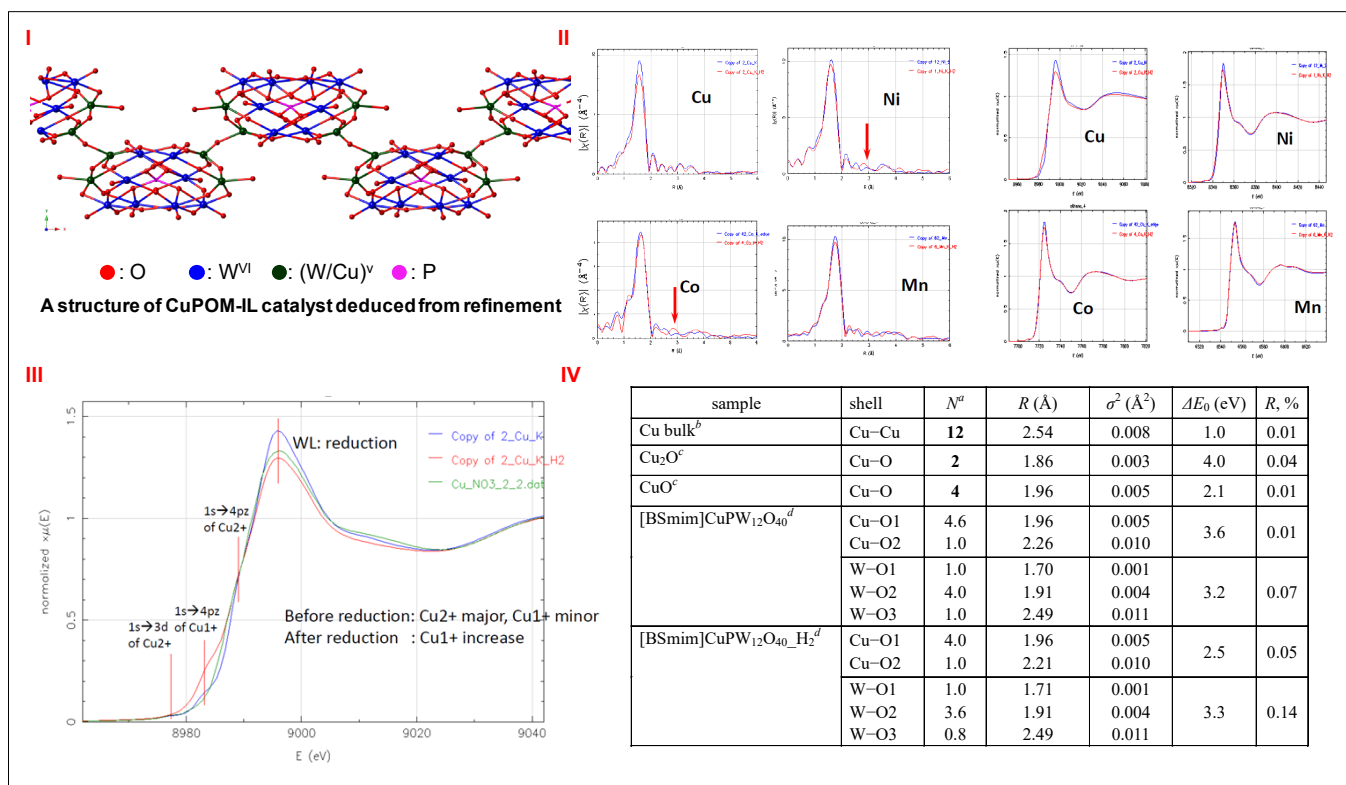


Figure 1. (I) The structure of CuPOM is obtained by transforming the space group *Pcca* to *Pncn* using winGX software, which was based on the Le Bail profile refinement data. The framework of CuPOM is using the ball-stick mode (Unit cell parameters illustrate in Supplementary Table S2); (II) EXAFS and XANES analyses of POM-ILs; (III) XANES analyses of [BSmim]CuPW₁₂O₄₀; (IV) Cu K-edge and W L₃-edge XAS analysis of [BSmim]CuPW₁₂O₄₀. ^a N , coordination number; R , distance between absorber and backscatter atoms; σ^2 , Debye–Waller factor to account for both thermal and structural disorders; ΔE_0 , inner potential correction; R factor (%) indicates the goodness of the fit. Error bounds (accuracies) that characterize the structural parameters obtained by EXAFS spectroscopy were estimated as $N \pm 20\%$; $R \pm 1\%$; $\sigma^2 \pm 20\%$; $\Delta E_0 \pm 20\%$. S_0^2 were determined from CuO and WO₃ standard fitting and fixed. Bold numbers indicate fixed coordination number (N) according to the crystal structure. O1, O2, and O3 represent the first, second, and third nearest neighbor coordination O atoms. ^b Fitting range: $2.5 \leq k$ (1/Å) ≤ 12.5 and $1.6 \leq R$ (Å) ≤ 2.8 . ^c Fitting range: $2.5 \leq k$ (1/Å) ≤ 12.5 and $1.0 \leq R$ (Å) ≤ 2.0 . ^d Cu K-edge fitting range: $2.9 \leq k$ (1/Å) ≤ 12.5 and $1.0 \leq R$ (Å) ≤ 2.6 ; W L₃-edge fitting range: $2.5 \leq k$ (1/Å) ≤ 14.5 and $1.0 \leq R$ (Å) ≤ 2.4 .

Additionally, XAS analysis (Figure 1II, III and Table S4) indeed shows that the oxidized CuPOM gives coordination number (CN) of around 6. Typically, Figure 1IV shows that the Cu^{2+} is in a distorted octahedral environment with CN of 5.6. This [BSmim]CuPW₁₂O₄₀ system displays the largest degree of reduction amongst all M studied (Table S4) with the Cu CN dropped to 5 in H₂ (reduced after H₂ pre-treatment at 200 °C to mimic the Cu^{2+} reduction in organic media) as well as the arisen of characteristic Cu^+ pre-edge peak at ~ 8984 eV and attenuation in white line signal at ~ 8996 eV in their XANES analysis (Figure 1II, III and Figure S4). The reduction can create vacant orbitals to facilitate the formation of di-oxygen activation from oxygen on activated ‘Cu’ in the reduced structure, as discussed. Cu substituted heteropolyoxometalates have many similarities to active Cu enzymes for O₂ transport/oxidation developed in biological systems, because they possess co-ordination sites surrounding an isolated Cu. End-on copper dioxygen adduct as ‘superoxo’ complexes have been proposed as reactive but selective intermediates in the catalytic cycle of mononuclear copper enzymes, such as peptidylglycine α -hydroxylating monooxygenase (PHM) or dopamine β -monooxygenase (DbH).²⁸ And indeed, the existence of such a species could be demonstrated by X-ray crystallography for a precatalytic PHM complex.²⁹ We believe that a similar superoxo is formed over the reduced Cu^+ in polyoxometalate in oxygen which selectively oxidizes lignin special linkages to give DEM in the catalytic process.

As shown in Table 1, a remarkably decline in lignin conversion (80.8%), volatile product yield (46.2 mg g⁻¹) and low DEM selectivity (23.8%) are exhibited using the ionic liquid [Bmim]CuPW₁₂O₄₀ without sulfonic group (Table 1, entry 8), which confirms that the acidic group in POM-IL is critical in lignin depolymerization. Further control experiment using H₂SO₄/CuSO₄ mixture catalyst results in very low selectivity of DEM (22.1%) and a sharp decrease in the yield of volatile products (Table 1, entry 9), elucidating clearly that polyoxometalate with ionic liquid cationic moiety is crucial during the

cleavage of lignin aromatic unit in ethanol. Interestingly, when a combined catalyst of CuSO_4 and $[\text{BSmim}]\text{Na}_2\text{PW}_{12}\text{O}_{40}$ is used, the yield of volatile products and DEM is far less than that of $[\text{BSmim}]\text{CuPW}_{12}\text{O}_{40}$ (Table 1, entry 7 vs. 10), but, in comparison with that of single catalyst $[\text{BSmim}]\text{Na}_2\text{PW}_{12}\text{O}_{40}$, an obvious enhancement of the catalytic activity is demonstrated (Table 1, entry 3 vs. 10). This can perhaps be attributed to a degree of *in situ* generation of $[\text{BSmim}]\text{CuPW}_{12}\text{O}_{40}$ from the ion exchange between Na^+ and Cu^{2+} . Furthermore, in the absence of oxygen, the lignin depolymerization is sharply decreased (Table 1, entry 11) with a conventional aromatic product distribution as that of acidic catalytic depolymerization (Table S6, entry 11). Moreover, when POM-IL catalyst is added, both weight-average molecular weight (M_w) and number-average molecular weight (M_n) of regenerated lignin (Table S6) are sharply decreased with comparison to those of original bagasse lignin samples (with the M_w and M_n values of 2698 and 1156, respectively). This demonstrates that lignin is depolymerized dramatically in an oxidation process using molecular oxygen from air as oxidant. Therefore, we can conclude that the significant promotion of the lignin depolymerization with oxidative cleavage of their benzene component is ascribed to the efficient synergistic effect between the acidic functional group, transition metal ion particularly Cu ion and miscible the polyoxometalate with lignin rather than any single factor.

Detailed investigation shows that appropriate POM-ILs content at elevated temperature and prolonged time can catalyze oxidative cleavage of lignin to DEM (Figure S7-S9). Also, the POM-IL catalyst shows the characteristic temperature controlling partition and recyclability (Figure S1): being miscible with reaction mixture at elevated temperature and precipitation at room temperature,³⁰ and no significant activity loss was observed after six runs (Figure S10). The effect of ethanol concentration seems to be critical, in which, the DEM yield and selectivity increase with increasing of ethanol concentration (Table 1, entry 12, Table S8, entries 1-6), yielding the maximum of 274.7 mg g⁻¹ and

69.0% selectivity to DEM in 100% ethanol. It suggests that ethanol can react *in situ* with the produced maleic acid to DEM and promote the lignin selective oxidation continuously. To obtain more evidence for this promotion, the reaction of maleic acid in ethanol-water was evaluated. The results show that all maleic acid can be converted at different concentrations of ethanol solvent. The DEM selectivity and yield can indeed reach 100% using pure ethanol (Table 1, entries 13-15; Table S8, entries 7-9). At the same time, the increase of the ethanol concentration can inhibit the generation of diethyl fumarate and diethyl malate, generating from the isomerization and hydration of maleic acid respectively (Table S8, entries 7-9). Therefore, this *in situ* esterification reaction is able to prevent the formed maleic acid from side reactions, which constitutes nearly the single DEM product formation.

In addition, we further measured the lignin carbon balance and C₉ unit utilization efficiency, which are generally key factors for lignin depolymerization,^{9,10} according to the results obtained from the optimized condition and the corresponding elemental analysis (Table S9). As shown in Figure 2, under the optimized condition (433 K for 5 h), 18.1% of the lignin carbon is converted to volatile products (Figure 2I), including 12.9% of DEM (Figure 2II). However, 56.4 % of lignin carbon is transformed into phenolic oligomer in this mild condition (Figure 2I), which is still recognized as a big challenge during lignin valorization due to its robust interunit linkage currently.^{3, 31} Interestingly, the phenolic oligomer from this POM-IL catalytic system can be further converted to DEM efficiently (Figure 2 and Table S10) when extra oxygen is presented. For example, the DEM yield sharply increases from 274.7 to 522.3 mg g⁻¹ with complete conversion of the lignin when extra 0.8 MPa oxygen is pressured and reheated for another 2 h. Namely, the carbon yield of DEM from lignin substantially increases from 12.9 to 24.5% with extra oxygen presence. C₉ unit utilization efficiency further illustrates that the converted lignin basic structure unit for DEM reach up to 24.5% and 55% with TON value 0.84 at the optimized condition and that with extra 0.8 MPa oxygen (Figure 2II). It is noteworthy that both of these

carbon utilization efficiencies to single chemical is much higher than that in many other lignin processes as well.^{3, 10, 31} Additionally, it indicates that insignificant change of lignin conversion and DEM selectivity are shown at various oxygen and nitrogen contents, 94.2% lignin conversion and 348.6 mg g⁻¹ DEM yield are achieved with 71.7% of the DEM selectivity under the mixture gas of 0.2 MPa N₂ and 0.8 MPa O₂ (Table S10, entry 5), and the gaseous fraction also exhibits a corresponding decrease in the oxygen content for the oxidation reaction (Table S11-S12). Therefore, it can be concluded safely that lignin carbon has a good utilization in this POM-IL catalytic system, implying its great potential in future lignin valorization.

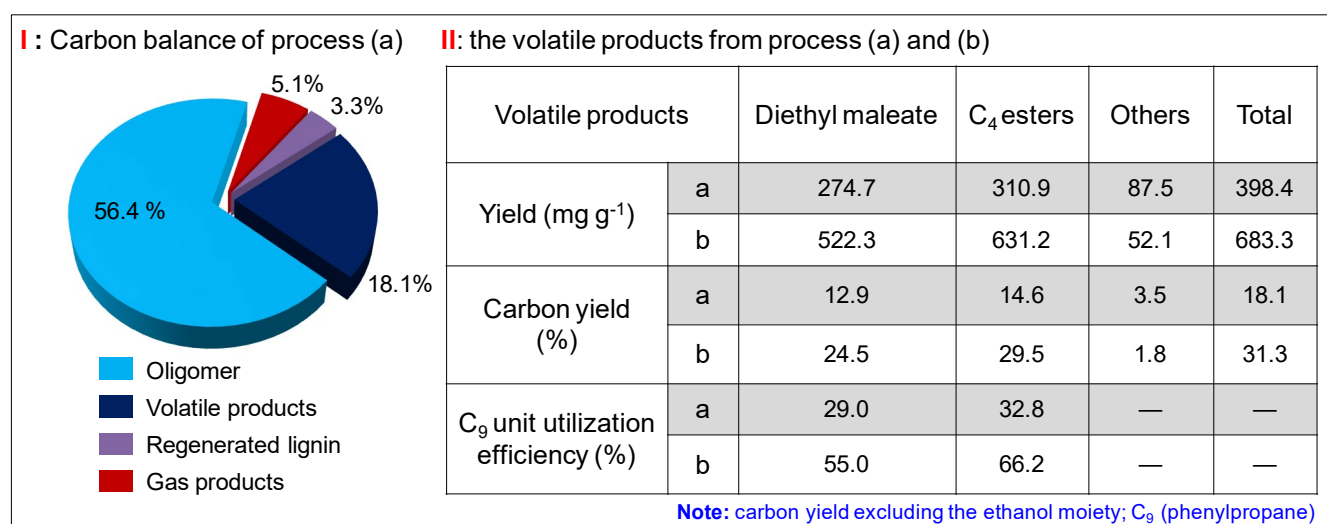


Figure 2. (I): Carbon balance of process (a); (II) the volatile products from process (a) and (b).

Reaction condition of process (a): 0.25 g bagasse lignin, 0.9 mmol [BSmim]CuPW₁₂O₄₀, 20 mL 100% ethanol, 433 K, 5 h, 0.8 MPa O₂; the process (b): purged by an extra 0.8 MPa oxygen when the reaction (a) was cooled to room temperature, and then heated to 433 K for another 2.0 h. Detailed calculation procedure can be found in the support information Eq.5 to Eq.10.

The adaptability of this POM-IL catalytic system is also checked with a series of typical feedstocks such as rice stalk lignin, pine lignin, corn stalk lignin, wheat stalk lignin and dealkaline lignin (Figure 3I, Table S13-S14). The results show that all lignin samples can be efficiently converted to DEM with high yield and selectivity. In particular, the wheat stalk lignin displays the highest volatile products yield of

556.7 mg g⁻¹ and DEM selectivity of 72.7%, which depicts an alternative route to the current butane technology for the DEM production.³² Furthermore, the efficient activity on dealkaline lignin sample (Figure 3I) indicates that this process of lignin conversion to DEM in ethanol is also applicable to those processed lignins from paper and pulp industry.

The evolution of lignin structure during the process

Comparative investigation on the structure evolution of bagasse lignin before and after reaction (original and regenerated lignin, respectively) was conducted using heteronuclear single quantum

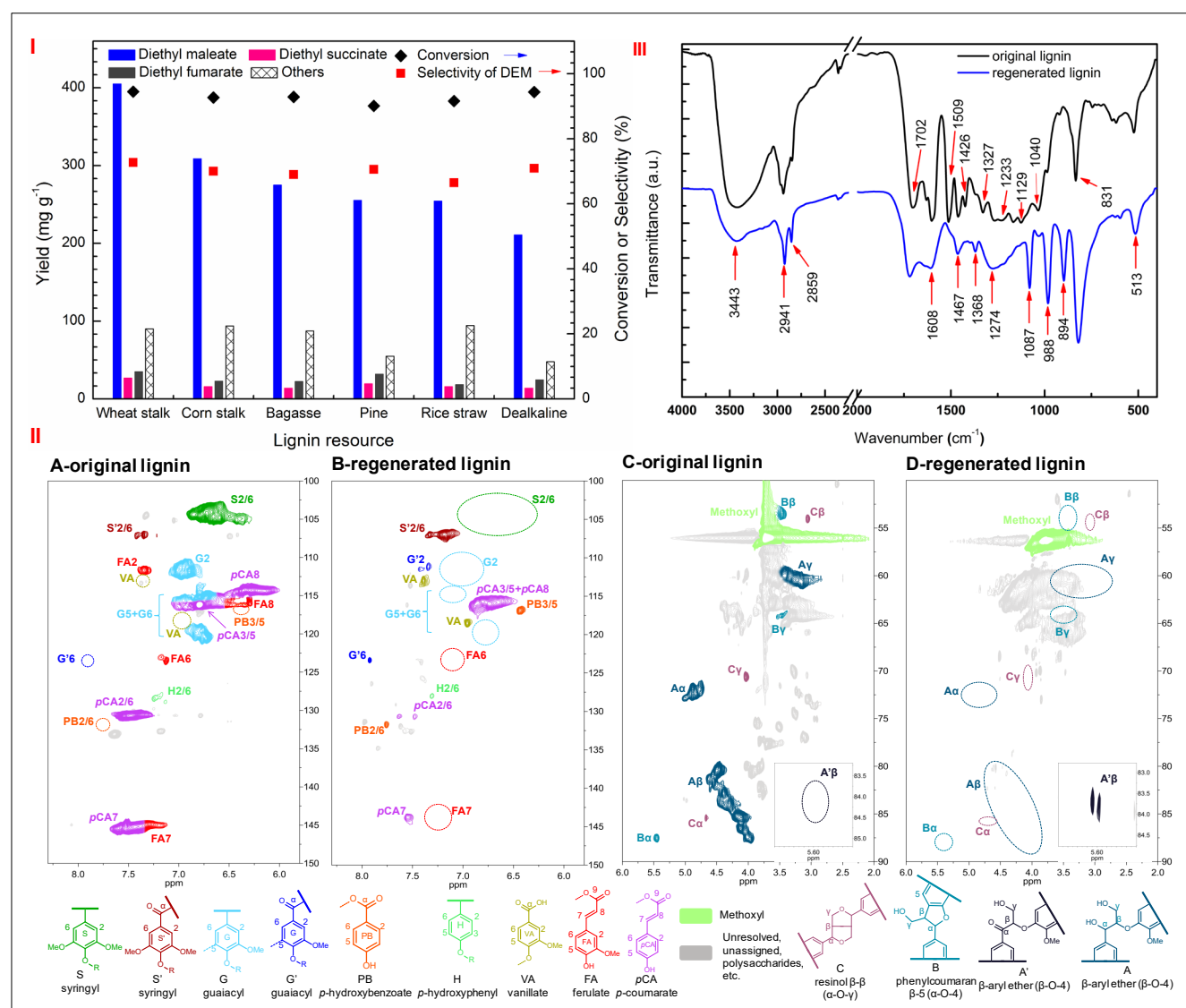


Figure 3. (I): The oxidative cleavage of lignin aromatic unit from various resources; (II): HSQC spectra of original (A, C) and regenerated bagasse lignin (B, D); (III) FT-IR spectra of original and regenerated bagasse lignin.

Reaction condition: 0.25 g lignin, 0.9 mmol [BSmim]CuPW₁₂O₄₀, 20 mL 100% ethanol, 433 K, 5 h, 0.8

MPa O₂.

correlation (HSQC). As shown in the aromatic regions (Figure 3II), typical basal structure units consist of methoxylated phenylpropanoid (syringyl and guaiacyl) subunits linked by β -O-4 (β -aryl ether) bonds referring as S and G³³ in the original lignin are disappeared completely after reaction, implying that S and G units are more flexible than the H unit for this lignin oxidative cleavage process catalyzed by the POM-ILs. This result is inconsistent with the previous studies where H is more active than G and S units in the lignin molecule cleavage,^{22, 34} indicating the different pathway for lignin conversion with POM-ILs. Besides, we also noticed that a small fraction of ketone S' and G'³³ is presented in the regenerated lignin. This can also be observed from the aliphatic regions, where the signals of branched chain are disappeared upon the uprising of ketone structure (Figure 3II). In Fourier Transform Infrared Spectra (FT-IR), absorption peaks representing condensed S plus G unit (1327 cm⁻¹) and typical S unit (1129 cm⁻¹)³⁵ are substantially weakened in that of regenerated lignin (Figure 3III and Table S15), indicating the efficient degradation of S and G units as well. However, it should be noticed that two new strong peaks at 1087 and 988 cm⁻¹ are appeared, which can be designated as the characteristic absorption of C=O and C-O valence vibration respectively,³⁶ further verifying the formation of G' and S' units. Additional, ¹³C-nuclear magnetic resonance (¹³C-NMR) analysis shows that the signals of 152.73, 130.74, 115.52 and 56.28, ppm, representing typical H, G, S lignin units, and -OCH₃, respectively,³⁷ are weakened in the regenerated lignin samples, demonstrating clearly the efficient lignin depolymerization, and the appearance of peak at 191.64 ppm indicated the formation of aromatic ketone (such as G' and S') during the process. Especially, the significantly declined signal at 56.28 ppm confirms that regenerated lignin contains less G and S units, further verifying that the H unit exhibits the lowest reactivity in this process (Figure S11).

Selective oxidation of model compound from lignin depolymerization

To gain further insight on the selectively oxidative cleavage of lignin aromatic unit to DEM, a series of phenol, guaiacol, syringol and their derivatives, the most representative chemicals from lignin depolymerization,^{3, 38} are used as model compounds. Excitedly, most of model compounds can be efficiently converted and exhibited relatively high yield and selectivity to DEM (Figure 4 and Table S16). However, the oxidative aromatic ring cleavage performances of these chemicals are dependent remarkably on the substituent groups of the monolignols. In the case of phenol (**1**), 251.8 mg g⁻¹ yield of total volatile products with 176.7 mg g⁻¹ of DEM is observed (Figure 4). When another hydroxyl group

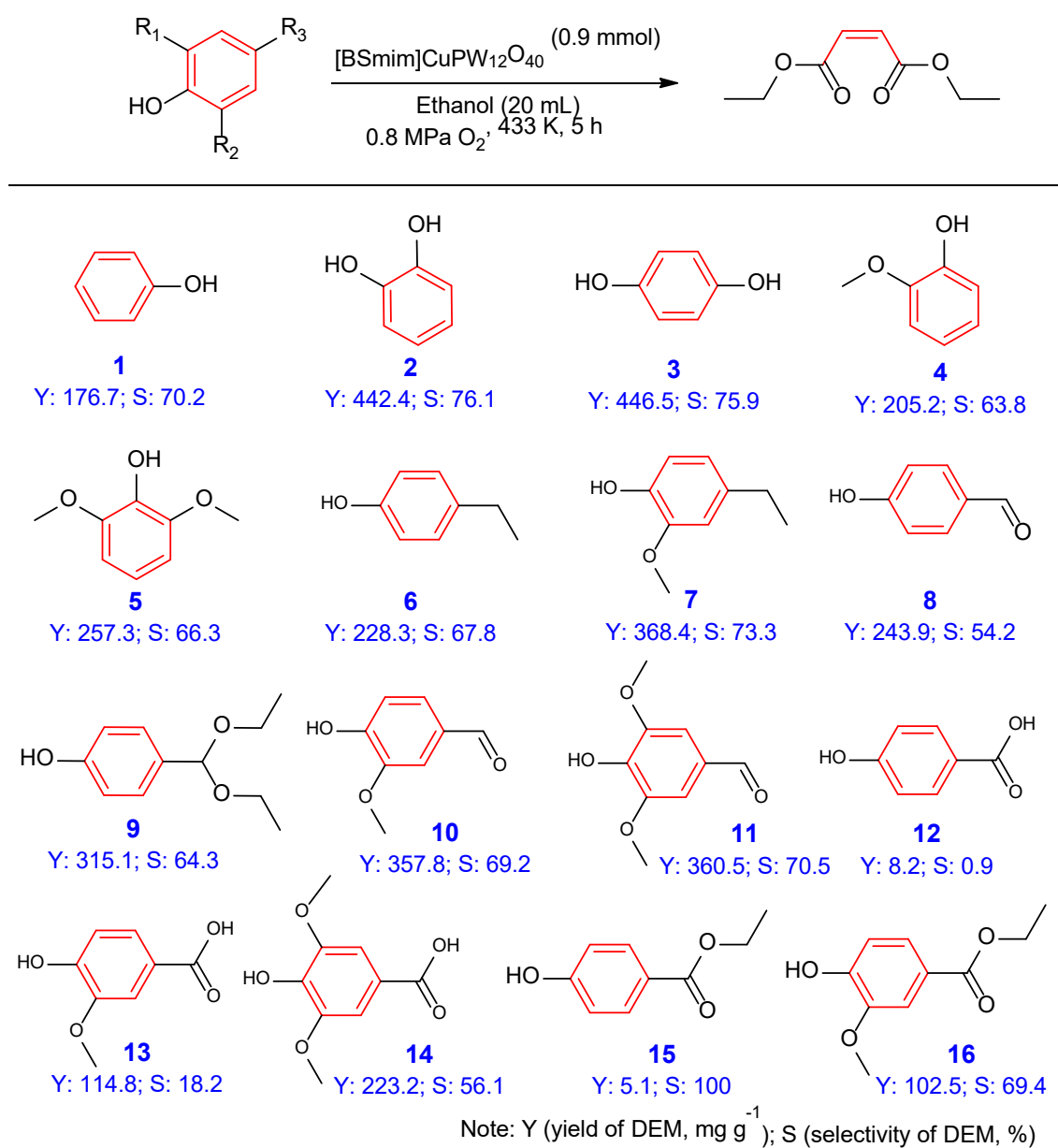


Figure 4. Catalytic oxidation of lignin model compounds into DEM

is introduced to either *ortho* or *para* position, the DEM yield sharply increases to 442.4 and 446.5 mg g⁻¹ respectively. It can be ascribed to the fact that both catechol and hydroquinol are more favorable to form benzoquinone, the intermediate of phenol oxidation and the key starting material for maleic acid generation.³⁹ Figure 4 also demonstrates that the oxidative ring cleavage of phenolic monomer is enhanced in the case of OCH₃-substituent at the *ortho* position (guaiacols (**4**) and syringols (**5**)). For example, the yields of total volatile products and DEM increase from 251.8 and 176.7 mg g⁻¹ to 321.6 and 205.2 mg g⁻¹, respectively when phenol is replaced by guaiacol. This increase is more remarkable when syringol is used, generating 388.1 and 257.3 mg g⁻¹ of total volatile product and DEM, respectively. It indicates that the depolymerization products from the G and S lignin are more facilitated to produce DEM than that of H lignin. This also explains well with the above comparative characterization between original and regenerated lignin, where more H structure unit is remained than G and S units (Figure 3II-III and Figure S11).

In general, the charge-density of the aromatic ring enhances with an electron donating substituent (such as ethyl and methoxyl groups) and weakens with an electron withdrawing substituent (such as aldehyde and carboxyl group).⁴⁰ Hence, the reactivity of aromatic ring and product regioselectivity are affected by the substituent in homogeneous phase reactions.^{33, 40} Here, higher charge density facilitates the oxidation of aromatic ring,⁴¹ resulting in higher DEM yield. For example, an electron donating methoxyl group in the *ortho* position of 4-ethyl phenol (**6**) by can elevate both the total product yield (from 336.7 to 502.4 mg g⁻¹) and DEM selectivity (from 67.8 to 73.3%, Table S16, entry 6 vs. 7). On the contrary, phenolic monomer with an electronic withdrawing substituent (for example, carboxyl and ester groups), a decrease of the oxidative ring cleavage is shown obviously due to the weakening of the electronic density of benzene skeleton (**12-16**). Aldehyde group is normally a stronger electron-drawing

group than carboxyl group.¹¹ However, it is very interesting that 4-hydroxybenzaldehyde (**8**), vanillin (**10**) and syringe aldehyde (**11**) show much higher activity than their corresponding acids and ester (Figure 4, model compound **12-16**), and it is even more active than the corresponding monolignols (Figure 4, phenol (**1**), guaiacol (**4**) and syringol (**5**) respectively). In this reaction, the aldehyde can condense quickly with ethanol catalyzed by acidic center of the catalyst. Therefore, the electron-drawing group of C=O in aldehyde is transformed to an electron donating group of -OC₂H₅ (This acetalization process can be verified by control process without O₂ addition), which results in the enhancement of the C-C bond cleavage of benzene ring. More evidence can be seen from Figure 4 as well, where the *p*-hydroxyl benzaldehyde (**8**) shows almost the same conversion nevertheless slightly less DEM yield than its corresponding acetal (**9**). And thus, the results about the selective oxidative ring cleavage of model chemicals clearly illustrate that lignin structure with more electron donating groups (such as -OCH₃) is much easier to be converted. Namely, G and S, the most predominant structure units in lignin,¹⁰ are more reactive than H, which accords well with the comparative characterization results of the lignin structure evolution. Finally, this result can be further confirmed by the conversion of several H-type dimers with typical linkages such as 4-O-5, α -O-4, 5-5, β -1. It can be seen from Table S16 that, the cleavages of C-O bonds such as 4-O-5 and α -O-4 *etc* are also effectively carried out, whereas, that of C-C bond remains insignificant because of its relatively higher activation energy. Based on above mentioned, we propose a plausible pathway for this efficient lignin depolymerization and oxidative ring cleavage (Figure S12), which can be further verified by the control experiments with several quinones as model compounds (Table S17).

In summary, a highly efficient and selective process for the production of DEM, an important, versatile and widely used bulk chemical from the fossil fuel currently, is achieved using POM-IL catalyst. Under optimized conditions, 94.5% of wheat stalk lignin is oxidized producing 556.7 mg g⁻¹ of

volatile products with a DEM selectivity of 72.7% over [BSmim]CuPW₁₂O₄₀. The presence of a significant synergistic effect between acidic functionalities and the superior activity of Cu ions in generating selective superoxo species within the polyoxometalate explains the observed improvement. Furthermore, the solvent of ethanol also shows an intensification effect on the DEM production, which substantially inhibits the further transformation of maleic acid and enhances the lignin conversion through its esterification with maleic acid to give unprecedented high yield of the single product. This process is highly feedstock adaptable for the depolymerization of many typical lignin sources with the significant advantage of facile catalyst separation and recycling by simple temperature control. Therefore, we have demonstrated that the present process has great potential in lignin valorization and sustainable DEM production due to its high process efficiency and DEM selectivity.

EXPERIMENTAL PROCEDURES

Full experimental procedures are provided in the Supplemental Information.

SUPPLEMENTAL INFORMATION

Supplemental Information includes Supplemental Experimental Procedures, 12 figures, and 17 tables and can be found with this article online.

AUTHOR CONTRIBUTIONS

C.Z.P, L.J.X, and L.X.H designed the catalysts and experiments, C.Z.P, L.Y.W, France J.L, and L.S.J synthesized and characterized the catalysts and conducted the experiments. Tsang. S.C.E performed the PXRD and XAS characterization and analysis with help from Y.L, D.J.C and Z.L.R. C.Z.P, L.J.X, France J.L, and L.X.H analyzed the data and wrote the manuscript with help from Tsang.S.C.E. Y.L, D.J.C, Z.L.R, Y.B.L and H.H.Y all gave contribution to catalysts characterization and products determination. All authors participated in data analyses and discussions.

ACKNOWLEDGMENTS

The financial support of the Natural Science Foundation of China (No, 21736003, 21336002, 21690083, 21878111, 21676108 and 11605225), the Science and Technology Program of Guangzhou, China (201804020014) and the Fundamental Research Funds for the Central Universities, SCUT are gratefully acknowledged. The access for beamline I11 of Diamond Light Source, UK for the SXRD characterization is acknowledged. The authors would like to thank Wenxing Chen of Tsinghua University, China for the help in sample preparation.

REFERENCES AND NOTES

1. Ragauskas, A.J., Beckham, G.T., Biddy, M.J., Chandra, R., Chen, F., Davis, M.F., Davison, B.H., Dixon, R.A., Gilna, P., Keller, M., et al. (2014). Lignin valorization: improving lignin processing in the biorefinery. *Science* 344, 709-719.
2. Rahimi, A., Ulbrich, A., Coon, J.J., and Stahl, S. S. (2014). Formic-acid-induced depolymerization of oxidized lignin to aromatics. *Nature* 515, 249-252.
3. Sun, Z., Fridrich, B., Santi, A.d., Elangovan, S., and Barta, K. (2018). Bright side of lignin depolymerization: toward new platform chemicals. *Chem. Rev.* 118, 614-678.
4. Wu, L., Moteki, T., Gokhale, A.A., Flaherty, D.W., and Toste, F.D. (2016). Production of fuels and chemicals from biomass: condensation reactions and beyond. *Chem* 1, 32-58.
5. Son, S., and Toste, F.D. (2010). Non-oxidative vanadium-catalyzed C-O bond cleavage: application to degradation of lignin model compounds. *Angew. Chem. Int. Ed.* 49, 3791-3794.
6. Lan, W., Amiri, M.T., Hunston, C.M., and Luterbacher, J.S. (2018). Protection group effects during α , γ -diol lignin stabilization promote high selectivity monomer production. *Angew. Chem. Int. Ed.* 57, 1356-1360.
7. Corma, A., Iborra, S., and Velty, A. (2007). Chemicals routes for the transformation of biomass into chemicals. *Chem. Rev.* 107, 2411-2502.

8. Guo, H., Zhang, B., Qi, Z., Li, C., Ji, J., Dai, T., Wang, A., and Zhang, T. (2017). Valorization of lignin to simple phenolic compounds over tungsten carbide: impact of lignin structure. *ChemSusChem* 10, 523-532.
9. Sun, Z., Fridrich, B., Santi, A.de., Elangovan, S., and Barta, K. (2018). Bright side of lignin depolymerization: toward new platform chemicals. *Chem. Rev.* 118, 614-678.
10. Li, C., Zhao, X., Wang, A., Huber, G.W., and Zhang, T. (2015). Catalytic transformation of lignin for the production of chemicals and fuels. *Chem. Rev.* 115, 11559-11624.
11. Suzuki, H., Cao, J., Jin, F., Kishita, A., Enomoto, H., and Moriya, T. (2006). Wet oxidation of lignin model compounds and acetic acid production. *J. Mater. Sci.* 41, 1591-1597.
12. Shuai, L., Amiri, M.T., Questell-Santiago, Y.M., Héroguel, F., Li, Y., Kim, H., Meilan, R., Chapple, C., Ralph, J., and Luterbacher, J.S. (2016). Formaldehyde stabilization facilitates lignin monomer production during biomass depolymerization. *Science* 354, 329-333.
13. Sun, N., Jiang, X., Maxim, M.L., Metlen, A., and Rogers, R.D. (2011). Use of polyoxometalate catalysts in ionic liquids to enhance the dissolution and delignification of woody biomass. *ChemSusChem* 4, 65-73.
14. Wang, M., Ma, J., Liu, H., Luo, N., Zhao, Z., and Wang, F. (2018). Sustainable productions of organic acids and their derivatives from biomass via selective oxidative cleavage of C-C bond. *ACS Catal.* 8, 2129-2165.
15. Zhao, X.B., and Zhu, J.Y. (2016). Efficient conversion of lignin to electricity using a novel direct biomass fuel cell mediated by polyoxometalates at low temperatures. *ChemSusChem* 9, 197-207.
16. Yadav, G.D., and Thathagar, M.B. (2002). Esterification of maleic acid with ethanol over cation-exchange resin catalysts. *React. Funct. Polym.* 52, 99-110.
17. Bernasconi, M., Muller, M. A., and Pfaltz, A. (2014). Asymmetric hydrogenation of maleic acid diesters and anhydrides. *Angew. Chem. Int. Ed.* 53, 5385-5388.

18. Coulston, G.W., Bare, S.R., Kung, H., Birkeland, K., Bethke, G.K., Harlow, R., Herron, N., and Lee, P.L. (1997).
The kinetic significance of V^{5+} in *n*-butane oxidation catalyzed by vanadium phosphates. *Science* 275, 191-193.
19. Dodds, D.R., and Gross, R.A. (2007). Chemicals from biomass. *Science* 318, 1250-1251.
20. Centi, G., Trifirò, F., Ebner, J.R., and Franchetti, V.M. (1988). Methanistic aspects of maleic anhydride synthesis
from C_4 hydrocarbons over phosphorus vanadium oxide. *Chem. Rev.* 88, 55-80.
21. Ma, R., Xu, Y., and Zhang, X. (2015). Catalytic oxidation of biorefinery lignin to value-added chemicals to
support sustainable biofuel production. *ChemSusChem* 8, 24-51.
22. Cai, Z., Li, Y., He, H., Zeng, Q., Long, J., Wang, L., and Li, X. (2015). Catalytic depolymerization of organosolv
lignin in a novel water/oil emulsion reactor: lignin as the self-surfactant. *Ind. Eng. Chem. Res.* 54, 11501-11510.
23. Wang, S., and Yang, G. (2015). Recent advances in polyoxometalate-catalyzed reactions. *Chem. Rev.* 115,
4893-4962.
24. Kozhevnikov, I.V. (1995). Heteropoly acids and related compounds as catalysts for fine chemical synthesis.
Catal. Rev. 37, 311-352.
25. Tadesse, H., and Luque, R. (2011). Advances on biomass pretreatment using ionic liquids: an overview. *Energ.*
Environ. Sci. 4, 3913–3929.
26. Spirlet, M.R., and Busing, W.R. (1978). Dodecatungstophosphoric acid-21-water by neutron diffraction. *Acta*
Crystallogr. B 34, 907-910.
27. Long, D. L., Burkholder, E., and Cronin, L. (2007). Polyoxometalate clusters, nanostructures and materials: from
selfassembly to designer materials and devices. *Chem. Soc. Rev.* 36, 105–121.
28. Mirica, L. M., Ottenwaelder, X., and Stack, T.D.P. (2004). Structure and spectroscopy of copper-dioxygen
complexes. *Chem. Rev.* 104, 1013-1046.
29. Prigge, S.T., Eipper, B.A., Mains, R.E., and Amzel, L.M. (2004). Dioxygen binds end-on to mononuclear copper
in a precatalytic enzyme complex. *Science* 304, 864-867.

30. Leng, Y., Wang, J., Zhu, D., Ren, X., Ge, H., and Shen, L. (2009). Heteropolyanion-based ionic liquids: reaction-induced self-separation catalysts for esterification. *Angew. Chem. Int. Ed.* 48, 168-171.
31. Schutyser, W., Renders, T., Bosch, S.V.d., Koelewijn, S.F., Beckham, G.T., and Sels, B.F. (2018). Chemicals from lignin: an interplay of lignocellulose fractionation, depolymerization, and upgrading. *Chem. Soc. Rev.* 47, 852-908.
32. Chen, B., and Munson, E.J. (2002). Investigation of the mechanism of *n*-butane oxidation on vanadium phosphorus oxide catalysts: evidence from isotopic labeling studies. *J. Am. Chem. Soc.* 124, 1638-1652.
33. Rahimi, A., Azarpira, A., Kim, H., Ralph, J., and Stahl, S.S. (2013). Chemoselective metal-free aerobic alcohol oxidation in lignin. *J. Am. Chem. Soc.* 135, 6415-6418.
34. Long, J., Lou, W., Wang, L., Yin, B., and Li, X. (2015). [C₄H₈SO₃Hmim]HSO₄ as an efficient catalyst for direct liquefaction of bagasse lignin: decomposition properties of the inner structural units. *Chem. Eng. Sci.* 122, 24-33.
35. Yan, T., Xu, Y., and Yu, C. (2009). The isolation and characterization of lignin of kenaf fiber. *J. Appl. Polym. Sci.* 114, 1896-1901.
36. Yang, Q., Wu, S., Lou, R., and Lv, G. (2011). Structural characterization of lignin from wheat straw. *Wood Sci. Technol.* 45, 419-431.
37. Sun, J., Sun, X., Sun, R., Fowler, P., and Baird, M.S. (2003). Inhomogeneities in the chemical structure of sugarcane bagasse lignin. *J. Agric. Food Chem.* 51, 6719-6725.
38. Lancefield, C.S., Ojo, O.S., Tran, F., and Westwood, N.J. (2015). Isolation of functionalized phenolic monomers through selective oxidation and C-O bond cleavage of the β -O-4 linkages in lignin. *Angew. Chem. Int. Ed.* 54, 258-262.
39. Santos, A., Yustos, P., Quintanilla, A., Rodríguez, S., and García-Ochoa, F. (2002). Route of the catalytic oxidation of phenol in aqueous phase. *Appl. Catal. B: Envir.* 39, 97-113.
40. Esguerra, K.V.N., Fall, Y., Petitjean, L., and Lumb, J-P. (2014). Controlling the catalytic aerobic oxidation of

phenols. *J. Am. Chem. Soc.* 136, 7662-7668.

41. Lee, J.Y., Peterson, R.L., Ohkubo, K., Garcia-Bosch, I., Himes, R.A., Woertink, J., Moore, C.D., Solomon, E.I., Fukuzumi, S., and Karlin, K.D. (2014). Mechanistic insights into the oxidation of substituted phenols via hydrogen atom abstraction by a cupric-superoxo complex. *J. Am. Chem. Soc.* 136, 9925-9937.